

Correlation effects as a Jahn-Teller phenomenon in mixed-valent semiconductors

O. Brandt

Institut für Theoretische Physik der Universität Stuttgart, Pfaffenwaldring 57, D-70550 Stuttgart, Germany

E. Sigmund

*Institut für Theoretische Physik der Universität Stuttgart, Pfaffenwaldring 57, D-70550 Stuttgart, Germany
and Institut für Physik, Technische Universität Cottbus, Karl Marx Straße 17, D-03046 Cottbus, Germany*

M. Wagner

*Institut für Theoretische Physik der Universität Stuttgart, Pfaffenwaldring 57, D-70550 Stuttgart, Germany
(Received 25 June 1993)*

In a previous study an unconventional species of a Jahn-Teller system was presented, where electronic excitations of the mixed-valent host crystal adopt the role which is usually played by nuclear displacements in the conventional coupling mechanism. In the present study the molecular model is extended to a doped-semiconductor model including an electronic transfer coupling. An electron capture in the defect states appropriate to describe electron spin resonance measurements of $\text{SmB}_6\text{:Gd}$ can be explained within this model by the formation of a band-gap state in the coupled system. The energetic lowering of a defect state as observed for $\text{SmB}_6\text{:Er}$ is examined, and is revealed to be most effective for a direct coupling to excitations of the localized $4f$ states of the Sm surrounding.

I. INTRODUCTION

The rare-earth compound SmB_6 has attracted intense theoretical and experimental interest as a mixed-valent prototype system. From experimental results it is accepted to be a semiconductor with an extremely small band gap of about 3–4 meV.^{1,2} This can be described as a hybridization gap between localized $4f$ and delocalized $5d$ orbitals including correlation effects.³ Not only does the ideal crystal show a variety of unusual properties but also doped ions in this material can show unexpected behavior. This was observed in electron spin resonance (ESR) spectra of the Gd^{3+} ,⁴ respectively, the Er^{3+} (Ref. 5) doped system.

At temperatures below about 5 K in the case of $\text{SmB}_6\text{:Gd}^{3+}$ a multiline spectrum was measured, which could not be explained by the $\text{Gd}(4f)^7$ configuration. With the hypothesis of an electron capture in an E_g crystal field state of the $\text{Gd}(5d)$ orbital at low temperatures, which results in a Gd^{2+} ground state, the spectrum could be interpreted. Above 6 K the anomalous spectrum vanished and the remaining lines could very well be related to the Gd^{3+} configuration. The mechanism of the electron attraction at the defect site remained unexplained. In the case of $\text{SmB}_6\text{:Er}^{3+}$ at 4.2 K an ESR spectrum was measured, which is related to a Γ_8 ground state instead of the expected Γ_6 state. The latter type of ground state is found in isostructural REB_6 compounds ($\text{RE}=\text{Ba}, \text{Ca}, \text{Yb}$), which show no mixed-valent behavior. Because of the remarkable isotropy of the lines the Γ_8 state of $\text{SmB}_6\text{:Er}^{3+}$ is not a pure crystal field state.

In both cases (Gd^{3+} , Er^{3+}) the relevant electronic defect states (E_g , Γ_8) are Jahn-Teller active because of their

spatial degeneracy. To take the mixed-valent surrounding into account, which offers “softer” electron (3–4 meV) than optical phonon (21 meV) excitations,⁶ a new type of Jahn-Teller mechanism was proposed for the Er^{3+} case.⁷ Thereby the defect states are coupled to electronic excitations of the host crystal. Thus the change in the electronic charge distribution of the surrounding atoms adopts the role of the nuclear distortions in the conventional Jahn-Teller system. In a molecular model of this mechanism the energetic lowering of the coupled Γ_8 state and the extraordinary isotropy of the Er^{3+} spectra could be explained.⁸

To receive a microscopic picture of the unconventional Jahn-Teller coupling we consider in this paper a doped semiconductor model. An electronic transfer between the defect states and the host crystal is included to examine the conditions of an electron capture in the case of $\text{SmB}_6\text{:Gd}$. In the second section we introduce a simplified model of the host crystal describing its essential electronic properties. In the third section we introduce the defect states and the relevant coupling mechanisms into this system. In the fourth section we calculate the defect Green function to determine the energetic position of the defect level for the Gd case, while in the fifth section a modified Hamiltonian for the Er case is considered.

II. HOST CRYSTAL SMB_6

The electronic properties of SmB_6 are determined by the degeneracy and the coupling of the two Sm configurations: $(4f)^6$ and $(4f)^5(5d)^1$. Since the $4f$ orbital is strongly localized, while the $5d$ orbital is delocalized, this

results in the mixing of a very narrow $4f$ and a broad $5d$ band in the crystal. In an octahedral surrounding, the former configuration leads to a singlet ground state, while the $4f$ part of the latter shows a twofold degenerate Γ_7 ground state. We consider in our model at each site of the cubic Sm sublattice two totally symmetric (A_{1g}) electronic levels, which are degenerate in the spin indices. One of these orbitals is supposed to be strongly localized, representing the $4f$ states, the other is delocalized and builds the broad $5d$ band. If we assume two particles at each site in the local limit of our model, the degree of degeneracy of the relevant Sm $4f$ configurations is reflected by the doubly occupied (singlet) configuration respectively, by a configuration where the localized level is singly occupied (twofold degenerate). Because the unoccupied localized state does not contribute to the mixed-valent behavior it has to be excluded. This is achieved by taking a Coulomb-like term into account which increases the energy of this configuration. The Hamiltonian describing the host crystal is a modified periodic Anderson model (H_{PAM}) (Ref. 9)

$$H_{\text{PAM}} = \sum_{\mathbf{k},\sigma} \varepsilon_{\mathbf{k}} d_{\mathbf{k}\sigma}^\dagger d_{\mathbf{k}\sigma} + \sum_{i\sigma} \varepsilon_f f_{i\sigma}^\dagger f_{i\sigma} + V \sum_{\mathbf{k},i,\sigma} \frac{1}{\sqrt{N}} [d_{\mathbf{k}\sigma}^\dagger f_{i\sigma} \exp(i\mathbf{k} \cdot \mathbf{R}_i) + \text{H.c.}] + \frac{1}{2} U \sum_{i,\sigma} f_{i\sigma} f_{i\sigma}^\dagger f_{i-\sigma} f_{i-\sigma}^\dagger, \quad (1)$$

$$\varepsilon_{\mathbf{k}} = 2t(\cos k_x + \cos k_y + \cos k_z). \quad (2)$$

The first term describes the broad pure $5d$ band with the nearest-neighbor dispersion relation $\varepsilon_{\mathbf{k}}$ and the operators $d_{\mathbf{k}\sigma}^\dagger, d_{\mathbf{k}\sigma}$. σ is the spin index and the \mathbf{k} sum runs over the first Brillouin zone (lattice constant $a=1$). The second term represents the strongly localized $4f$ states with the potential energy ε_f lying within the range of the $5d$ band (operators $f_{i\sigma}^\dagger, f_{i\sigma}$). The third term shows the $4f$ - $5d$ mixing leading to hybridization. The last term can be used to describe SmB_6 .¹⁰ With the use of the anticommutator relations the corresponding operator is transformed to $(1 - f_{i\sigma}^\dagger f_{i\sigma})(1 - f_{i-\sigma}^\dagger f_{i-\sigma})$. It therefore leads to an energetic increase of the unoccupied localized level.

We change into the picture of holes ($f_{i\sigma}^\dagger \rightarrow f_{hi\sigma}$, $d_{\mathbf{k}\sigma}^\dagger \rightarrow d_{hk\sigma}$) and consider the limit $U \rightarrow \infty$. In this case the occupancy of the localized level with two holes is excluded and we can apply the slave boson approach.^{11,12} The Bose field with zero energy is described by the operators b_i^\dagger, b_i . The following constraint for the hole occupation numbers of the localized states and the Bose field at each lattice site results in the exclusion of the doubly occupied localized level in the hole picture.

$$\sum_{\sigma} f_{hi\sigma}^\dagger f_{hi\sigma} + b_i^\dagger b_i = 1. \quad (3)$$

Consistent with this restriction the following Hamiltonian corresponding to Eq. (1) is obtained:

$$H_{SB} = \sum_{\mathbf{k},\sigma} \varepsilon_{\mathbf{k}} (1 - d_{hk\sigma}^\dagger d_{hk\sigma}) + \sum_{i\sigma} \varepsilon_f (1 - f_{hi\sigma}^\dagger f_{hi\sigma}) - V \sum_{\mathbf{k},i,\sigma} \frac{1}{\sqrt{N}} [f_{hi\sigma}^\dagger b_i d_{hk\sigma} \exp(i\mathbf{k} \cdot \mathbf{R}_i) + \text{H.c.}] \quad (4)$$

and Eq. (3) adopts the role of a subsidiary condition to (4). Characteristic electronic properties of the crystal are already described within the mean field approximation for the bosonic operators, where these are replaced by their expectation value ($r = \langle b^\dagger \rangle = \langle b \rangle$). Within this approximation the Hamiltonian including the constraint (3) with a Lagrange multiplier Λ_{SB} reads

$$\tilde{H}_{SB} = - \sum_{\mathbf{k}\sigma} \varepsilon_{\mathbf{k}} d_{hk\sigma}^\dagger d_{hk\sigma} - \sum_{\mathbf{k},\sigma} \tilde{\varepsilon}_f f_{hk\sigma}^\dagger f_{hk\sigma} - \sum_{\mathbf{k}\sigma} \frac{1}{\sqrt{N}} \tilde{V} (f_{hk\sigma}^\dagger d_{hk\sigma} + \text{H.c.}) + \Lambda_{SB} N (r^2 - 1) + \sum_{\mathbf{k}\sigma} (\varepsilon_{\mathbf{k}} + \varepsilon_f), \quad (5)$$

$$\tilde{\varepsilon}_f = \varepsilon_f - \Lambda_{SB}, \quad \tilde{V} = Vr. \quad (6)$$

In (6) $f_{hk\sigma}^\dagger = \sum_i \frac{1}{\sqrt{N}} \exp(i\mathbf{k} \cdot \mathbf{R}_i) f_{hi\sigma}^\dagger$ was used. A self-consistent solution is received by exploiting the Bogoliubov-Feynman inequality for the free energy of a test Hamiltonian.¹³ This leads to the self-consistency equations

$$\bar{n}_{fh} + r^2 = 1, \quad (7)$$

$$\bar{n}_{fh} = \sum_{\mathbf{k},\sigma} \frac{1}{N} \left\langle f_{hk\sigma}^\dagger f_{hk\sigma} \right\rangle_T^{\tilde{H}_{SB}}, \quad (8)$$

$$2\Lambda_{SB} r = \sum_{\mathbf{k},\sigma} \frac{1}{N} \left\langle f_{hk\sigma}^\dagger d_{hk\sigma} + \text{H.c.} \right\rangle_T^{\tilde{H}_{SB}}, \quad (9)$$

where $\langle \rangle_T^{\tilde{H}_{SB}}$ denotes the thermal expectation value with respect to \tilde{H}_{SB} . To diagonalize the Hamiltonian we make use of the transformation

$$c_{hk1\sigma}^\dagger = \gamma_{\mathbf{k}}^* d_{hk\sigma}^\dagger + \beta_{\mathbf{k}}^* f_{hk\sigma}^\dagger, \quad (10)$$

$$c_{hk2\sigma}^\dagger = \beta_{\mathbf{k}}^* d_{hk\sigma}^\dagger - \gamma_{\mathbf{k}}^* f_{hk\sigma}^\dagger,$$

where the coefficients obey $|\beta_{\mathbf{k}}|^2 + |\gamma_{\mathbf{k}}|^2 = 1$ and $\beta_{\mathbf{k}} \gamma_{\mathbf{k}}^* + \beta_{\mathbf{k}}^* \gamma_{\mathbf{k}} = 0$ to fulfill the anticommutator relations for Fermi operators. When we choose $\gamma_{\mathbf{k}}$ and $\beta_{\mathbf{k}}$ as

$$\gamma_{\mathbf{k}} = \left[\frac{1}{2} \left(1 - \frac{\varepsilon_{\mathbf{k}} - \tilde{\varepsilon}_f}{W_{\mathbf{k}}} \right) \right]^{\frac{1}{2}}, \quad (11)$$

$$\beta_{\mathbf{k}} = - \left[\frac{1}{2} \left(1 + \frac{\varepsilon_{\mathbf{k}} - \tilde{\varepsilon}_f}{W_{\mathbf{k}}} \right) \right]^{\frac{1}{2}} \text{sgn}(\tilde{V}),$$

$$W_{\mathbf{k}} = \left[(\varepsilon_{\mathbf{k}} - \tilde{\varepsilon}_f)^2 + 4\tilde{V}^2 \right]^{\frac{1}{2}}, \quad (12)$$

Eq. (5) is diagonalized. Thus a hybridized band structure (band index 1) is described, degenerate in the spin indices. We write down the resulting Hamiltonian in

the conventional picture of electronic operators ($c_{hkl\sigma} \rightarrow c_{kl\sigma}^\dagger, c_{hkl\sigma}^\dagger \rightarrow c_{kl\sigma}$),

$$\tilde{H}_{SB} = \sum_{\mathbf{k}, l, \sigma} \varepsilon_{kl} c_{kl\sigma}^\dagger c_{kl\sigma} + \Lambda_{SB} N(r^2 + 1), \quad (13)$$

$$\varepsilon_{\mathbf{k}1} = \frac{1}{2}(\tilde{\varepsilon}_f + \varepsilon_{\mathbf{k}} - W_{\mathbf{k}}),$$

$$\varepsilon_{\mathbf{k}2} = \frac{1}{2}(\tilde{\varepsilon}_f + \varepsilon_{\mathbf{k}} + W_{\mathbf{k}}). \quad (14)$$

Because the system is bilinear within this approximation the expectation values in Eqs. (7) and (8) can easily be evaluated, yielding the self-consistency equations (7) – (9) in the form

$$r^2 = 1 - \bar{n}_{fh}, \quad (15)$$

$$\bar{n}_{fh} = 2 \frac{1}{N} \sum_{\mathbf{k}} \left\{ |\beta_{\mathbf{k}}|^2 \left[1 - f(\varepsilon_{\mathbf{k}1}, T) \right] + |\gamma_{\mathbf{k}}|^2 \left[1 - f(\varepsilon_{\mathbf{k}2}, T) \right] \right\}, \quad (16)$$

$$\Lambda_{SB} = \frac{2V}{rN} \sum_{\mathbf{k}} \gamma_{\mathbf{k}} \beta_{\mathbf{k}} \left[f(\varepsilon_{\mathbf{k}2}, T) - f(\varepsilon_{\mathbf{k}1}, T) \right].$$

$f(\varepsilon_{\mathbf{k}l}, T)$ is the Fermi-Dirac distribution function. The chemical potential μ and the parameters r and Λ_{SB} were determined self-consistently. Because of the given particle number (two electrons per site) this results in a semiconductor with a small band gap. In Fig. 1 the dispersion relation of the system is drawn for the self-consistent (full line, $U \rightarrow \infty$) and the corresponding tight-binding calculation (dotted lines, $U = 0$). The effective one-particle Hamiltonian leads to an energetic lowering of the localized $4f$ level and, because of the reduction of the mixing constant \tilde{V} , to a decrease in the size of the band gap. The energetic lowering for the Sm compound is in contrast to the energetic raising of the localized level in the case of the corresponding calculation for Ce compounds.¹³ In the effective one-particle picture this reflects the fact that in the former case the unoccupied localized states are excluded, while in the latter the excluded states are the doubly occupied ones.

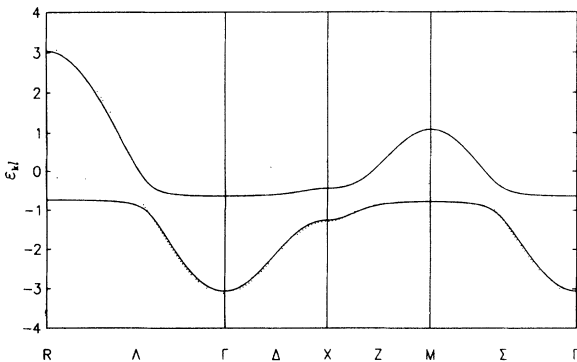


FIG. 1. Comparison between the self-consistently calculated band structure of our model of SmB₆ (full line) and the corresponding tight-binding model (dotted line). —, $\tilde{\varepsilon}_f = -0.7$, $\tilde{V} = 0.38$, $U \rightarrow \infty$; ·····, $\varepsilon_f = 0.05$, $V = 0.6$, $U = 0$.

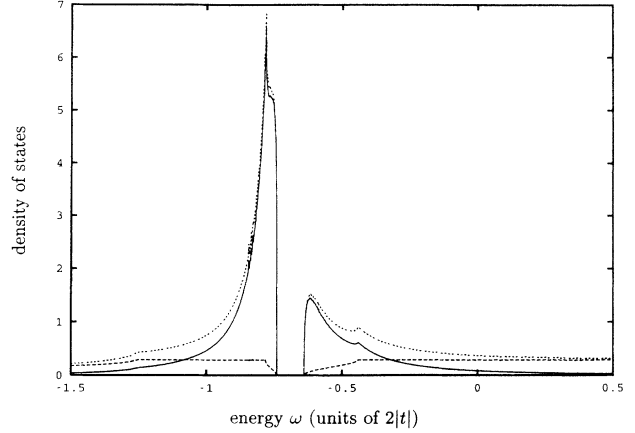


FIG. 2. Total density of states (DOS) (arb. units, dotted line), partial DOS of localized $4f$ states (full line), and partial DOS of delocalized $5d$ states (interrupted line) of the model for SmB₆. $\tilde{\varepsilon}_f = -0.7$; $\tilde{V} = 0.38$.

In Fig. 2 the total density of states (dotted line), the $4f$ density of states (full line), and the $5d$ partial density of states (interrupted line) are shown. The sharp maxima near the band gap are formed by the $4f$ states, while the $5d$ states constitute the flat background of the hybridized band. In our model the hybridized band structure is determined by the parameters $t = -0.5$, $\tilde{V} = 0.38$, and $\tilde{\varepsilon}_f = -0.7$ in units of $2|t| = 1$ eV. This results in $\bar{n}_{fh} = 0.63$, which is consistent with the measured Sm valence of 2.6 to 2.7, but leads to a band gap E_{gap} which is too large by an order of magnitude. The parameters were chosen to make numerical integrations in the following sections feasible; they give a qualitatively correct density of states of the host crystal.

III. DEFECT MODEL HAMILTONIAN

In our model we consider a defect representing a Gd or an Er ion, which substitutes a Sm ion and therefore obeys octahedral symmetry. To keep the model simple we assume at the defect site two A_{1g} states with the same physical properties as the replaced Sm states and additionally a Jahn-Teller active E_g orbital. Because only spatial degrees of freedom are relevant in our coupling we neglect the spin indices. In this way the Γ_3 state can represent both the Gd $5d$ crystal field state and the spatial part of the Er Γ_8 state.

We assume local coupling of the defect states to the nearest-neighbor Sm states, which form the irreducible representations $2A_{1g}$, $2E_g$, and $2T_{1u}$. The Jahn-Teller coupling of the E_g defect states can be established by transitions between A_{1g} and E_g states of the surrounding. We can consider various coupling types, which differ mainly in respect to the spatial extent of the involved local Sm states. This is discussed in Sec. VI. In the following we consider the Jahn-Teller coupling to the localized Sm states. To examine the electron capture we include in our model an electron transfer between the E_g defect states and that E_g state of the surrounding which is built up by delocalized Sm states.

The Hamiltonian for the doped semiconductor model now reads

$$H = H_0 + H_{t_d} + H_\lambda, \quad (17)$$

$$H_0 = \sum_{\kappa} \tilde{\varepsilon}_{\kappa} c_{\kappa}^{\dagger} c_{\kappa} + \sum_{i=1,2} \tilde{\varepsilon}_0 a_i^{\dagger} a_i, \quad (18)$$

$$\begin{aligned} H_{t_d} &= t_d \left(C_1^{\dagger} a_1 + C_2^{\dagger} a_2 + \text{H.c.} \right) \\ &= t_d \sum_{\kappa} \left[\xi_{1t_d}(\kappa) c_{\kappa}^{\dagger} a_1 + \xi_{2t_d}(\kappa) c_{\kappa}^{\dagger} a_2 + \text{H.c.} \right], \quad (19) \end{aligned}$$

$$\begin{aligned} H_\lambda &= \lambda \left[\left(C_0^{\dagger} C_1 + C_1^{\dagger} C_0 \right) \left(a_2^{\dagger} a_2 - a_1^{\dagger} a_1 \right) \right. \\ &\quad \left. + \left(C_0^{\dagger} C_2 + C_2^{\dagger} C_0 \right) \left(a_2^{\dagger} a_1 + a_1^{\dagger} a_2 \right) \right] \\ &= \lambda \sum_{\kappa, \kappa'} \left(c_{\kappa}^{\dagger} c_{\kappa'} + c_{\kappa'}^{\dagger} c_{\kappa} \right) \\ &\quad \times \left[\xi_0(\kappa) \xi_1(\kappa') \left(a_2^{\dagger} a_2 - a_1^{\dagger} a_1 \right) \right. \\ &\quad \left. + \xi_0(\kappa) \xi_2(\kappa') \left(a_2^{\dagger} a_1 + a_1^{\dagger} a_2 \right) \right]. \quad (20) \end{aligned}$$

H_0 describes the mixed-valent semiconductor ($\kappa = \mathbf{kl}$) and the degenerate E_g states with the potential energy $\tilde{\varepsilon}_0$ and the operators a_i^{\dagger} , respectively, a_i ($i = 1, 2$). The tilde signifies that the energy values are related to μ . H_{t_d} allows the transfer of an electron between the defect states and those of Sm neighbors. H_λ describes the correlation coupling mechanism of the defect states to A_{1g} - E_g transitions. The operators of the A_{1g} states C_0^{\dagger} (C_0) and those of the E_g states $C_1^{\dagger}, C_2^{\dagger}$ (C_1, C_2) are defined by

$$C_0^{\dagger} = \frac{1}{\sqrt{6}} \left(f_{\hat{x}}^{\dagger} + f_{-\hat{x}}^{\dagger} + f_{\hat{y}}^{\dagger} + f_{-\hat{y}}^{\dagger} + f_{\hat{z}}^{\dagger} + f_{-\hat{z}}^{\dagger} \right), \quad (21)$$

$$C_1^{\dagger} = \frac{1}{\sqrt{12}} \left(2f_{\hat{z}}^{\dagger} + 2f_{-\hat{z}}^{\dagger} - f_{\hat{x}}^{\dagger} - f_{-\hat{x}}^{\dagger} - f_{\hat{y}}^{\dagger} - f_{-\hat{y}}^{\dagger} \right)$$

$$C_2^{\dagger} = \frac{1}{2} \left(f_{\hat{x}}^{\dagger} + f_{-\hat{x}}^{\dagger} - f_{\hat{y}}^{\dagger} - f_{-\hat{y}}^{\dagger} \right). \quad (22)$$

\hat{x} , \hat{y} and \hat{z} establish the base of the simple cubic Sm lattice. Because in H_{t_d} the delocalized Sm states are involved the operators f_i^{\dagger} in Eq. (22) have to be replaced by the operators d_i^{\dagger} in the definition of $C_1^{\dagger}, C_2^{\dagger}$ (C_1, C_2) of the transfer operator. The operators of the Sm states are expanded into terms of the operators of the band system, yielding the corresponding coefficients ξ_0, ξ_1 , and ξ_2 .

IV. GD DEFECT CASE

We are interested in the energetic position of the coupled defect level. This is easily revealed by the one-particle Zubharev Green function, because its imaginary part yields the corresponding partial density of states. The Green function was calculated by means of Mori's formalism. For this purpose it is reasonable to define the Mori scalar product

$$(A|B) \equiv \langle AB^{\dagger} + B^{\dagger}A \rangle_T. \quad (23)$$

The link between the anticommutator Green function in Fourier space and the Mori scalar product in Laplace space then reads

$$\langle \langle A|A^{\dagger} \rangle \rangle_E = \frac{-i}{2\pi} \left(\frac{1}{z - i\mathcal{L}} A|A \right)_{z=-iE}, \quad (24)$$

$$\mathcal{L} = [H, \dots],$$

$$E = \omega \pm i\epsilon, \quad \hbar = 1. \quad (25)$$

The evaluation of the scalar product in this equation is determined by Mori's evolution equation

$$\left(\frac{1}{z - i\mathcal{L}} A|A \right) = \frac{(A|A)}{z - i\omega_0 + \tilde{M}(z)}, \quad (26)$$

where

$$\omega_0 = (\mathcal{L}A|A) (A|A)^{-1}, \quad (27)$$

$$\tilde{M}(z) = \left(\frac{1}{z - Q\mathcal{L}Q} Q\mathcal{L}A|Q\mathcal{L}A \right) (A|A)^{-1}, \quad (28)$$

$$Q = 1 - P, \quad (29)$$

$$PX = (X|A) (A|A)^{-1} A. \quad (30)$$

In this section we choose the observable $A = a_i$ ($i = 1, 2$). The static scalar product therefore results in $(A|A) = 1$. ω_0 and $\tilde{M}(z)$ cannot be determined exactly in the considered model. In this section we take terms to second order in $w = t_d, \lambda$ into account and factorize the appearing thermal expectation values under the assumption that κ is still a good quantum number. To calculate ω_0 and $\tilde{M}(z)$ we subdivide \mathcal{L} according to the parts H_0, H_{t_d} , and H_λ in our Hamiltonian and find

$$\mathcal{L}^0 a_i = -\tilde{\varepsilon}_0 a_i, \quad (31)$$

$$\mathcal{L}^{t_d} a_i = -t_d \sum_{\kappa} \left[\xi_{1,t_d}(\kappa) \delta_{i,1} + \xi_{2,t_d}(\kappa) \delta_{i,2} \right] c_{\kappa}, \quad (32)$$

$$\begin{aligned} \mathcal{L}^{\lambda} a_i &= -\lambda \sum_{\kappa, \kappa'} \left(c_{\kappa}^{\dagger} c_{\kappa'} + c_{\kappa'}^{\dagger} c_{\kappa} \right) \\ &\quad \times \left[\xi_0(\kappa) \xi_1(\kappa') \left(a_2 \delta_{i,2} - a_1 \delta_{i,1} \right) + \xi_0(\kappa) \xi_2(\kappa') \right. \\ &\quad \left. \times \left(a_2 \delta_{i,1} - a_1 \delta_{i,2} \right) \right]. \quad (33) \end{aligned}$$

To obtain ω_0 we need the scalar products

$$(\mathcal{L}^0 a_i | a_i) = -\tilde{\varepsilon}_0, \quad (34)$$

$$(\mathcal{L}^{t_d} a_i | a_i) = 0, \quad (35)$$

$$\begin{aligned} (\mathcal{L}^{\lambda} a_i | a_i) &= r - \lambda \sum_{\kappa, \kappa'} \left\langle c_{\kappa} c_{\kappa'}^{\dagger} + c_{\kappa'}^{\dagger} c_{\kappa} \right\rangle_T \xi_0(\kappa) \xi_1(\kappa') \\ &\quad \times (\delta_{i,2} - \delta_{i,1}). \quad (36) \end{aligned}$$

Within our approximation $(\mathcal{L}^{\lambda} a_i | a_i)$ vanishes, because of the symmetry of the coupling coefficients. This yields

$$\omega_0 = -\tilde{\varepsilon}_0. \quad (37)$$

Since we are interested in terms in order w^2 and since $Q\mathcal{L}A_i$ is of order w , we can replace $Q\mathcal{L}Q$ in the resolvent

of $\tilde{M}(z)$ by \mathcal{L} . This leads to the following expression for the self-energy $\tilde{M}(E) = -i\tilde{M}(z = -iE)$:

$$\tilde{M}(E) = \tilde{M}_{t_d}(E) + \tilde{M}_\lambda(E), \quad (38)$$

$$\tilde{M}_{t_d}(E) = t_d^2 \sum_{\kappa} \frac{\xi_{1t_d}^2(\kappa)\delta_{i,1} + \xi_{2t_d}^2(\kappa)\delta_{i,2}}{E - \tilde{\varepsilon}_\kappa}, \quad (39)$$

$$\begin{aligned} \tilde{M}_\lambda(E) = & \lambda^2 \sum_{\kappa, \kappa'} \frac{\xi_0^2(\kappa)\xi_E^2(\kappa') + \xi_E^2(\kappa)\xi_0^2(\kappa')}{E - \tilde{\varepsilon}_0 - \tilde{\varepsilon}_{\kappa'} + \tilde{\varepsilon}_\kappa} \\ & \times \left[\left\langle c_\kappa^\dagger c_\kappa \right\rangle_T \left(1 - \left\langle c_{\kappa'}^\dagger c_{\kappa'} \right\rangle_T \right) + \left\langle a_i^\dagger a_i \right\rangle_T \right. \\ & \left. \times \left(\left\langle c_{\kappa'}^\dagger c_\kappa \right\rangle_T - \left\langle c_\kappa^\dagger c_{\kappa'} \right\rangle_T \right) \right], \end{aligned} \quad (40)$$

$$\xi_E^2(\kappa) = \xi_1^2(\kappa) + \xi_2^2(\kappa). \quad (41)$$

By means of (24) the Green function of the defect level then reads

$$\langle\langle a_i | a_i^\dagger \rangle\rangle_E = \frac{1}{2\pi} \frac{1}{E - \tilde{\varepsilon}_0 - \tilde{M}(E)}. \quad (42)$$

The self-energy part \tilde{M}_{t_d} is well known from the Fano-resonance problem.¹⁴ It leads to a shift of the defect level depending on the position of $\tilde{\varepsilon}_0$ with respect to the band structure. In the self-energy part \tilde{M}_λ the many-body character of the coupling is reflected in the appearance of occupation probabilities of the band states and of the defect level. Since we consider only one defect site within the host crystal the change in the energy values of the band states with respect to the uncoupled values is of order $1/N$. Therefore we introduce the approximation $\langle c_\kappa^\dagger c_\kappa \rangle_T \approx f(\tilde{\varepsilon}_\kappa, T)$. The remaining expectation value $\langle a_i^\dagger a_i \rangle_T$ is determined by use of the spectral function

$$\begin{aligned} \langle a_i^\dagger a_i \rangle_T = & \int_{-\infty}^{+\infty} d\omega \frac{i}{\exp(\beta\omega) + 1} \left[\langle\langle a_i | a_i^\dagger \rangle\rangle_{\omega+i\epsilon} \right. \\ & \left. - \langle\langle a_i | a_i^\dagger \rangle\rangle_{\omega-i\epsilon} \right]. \end{aligned} \quad (43)$$

The considered Green function describes a “test particle” (electron or hole) in the defect state added to the semiconducting system. If we assume that the uncoupled defect level is situated in the conduction band, the considered electron for $T = 0$ suffers an energetic lowering, which essentially is caused by the correlation coupling. Since the doubly occupied defect state shows A_2 symmetry, the Jahn-Teller coupling is only efficient for the singly occupied state. Therefore the energetic lowering of the defect level into the range of the valence band is not allowed. In our calculation this unphysical behavior is excluded by the self-consistent determination of $\langle a_i^\dagger a_i \rangle$.

Our physical picture of the electron capture in the Gd case now is the following. If the uncoupled defect level is lying near the band gap within the conduction band the Jahn-Teller coupling can shift the level into the band gap. In this case $\text{Im}\tilde{M}_{t_d}(\omega)$ vanishes because $\xi_{it_d}^2 = 0$ within the gap, while $\text{Im}\tilde{M}_\lambda(\omega)$ is zero for $\omega < \tilde{\varepsilon}_0 + E_{\text{gap}}$ and $\langle a_i^\dagger a_i \rangle_T \sim 0$. Therefore a sharply peaked contribution to

the density of states appears. Because the three-valent Gd introduces an electron into the conduction band, this electron will be captured in the energetically lowered defect level within the band gap.

In Fig. 3 the imaginary part of the Green function is shown for $\tilde{\varepsilon}_0 + \mu = \varepsilon_0 = -0.56$ and $t_d = 0.25$. For $\lambda = 0$ the maximum within the conduction band is broadened because of the transfer coupling (interrupted line). The Jahn-Teller coupling, however, leads to a sharp peak within the band gap (full line, $\lambda = 0.25$) for $\lambda > \lambda_c$, where λ_c depends on t_d and $\tilde{\varepsilon}_0$.

In Fig. 4 we show the temperature dependency of the self-energy in the one-pole approximation $\text{Re}\tilde{M}_\lambda(\omega = \tilde{\varepsilon}_0)$, which determines in a good approximation the energetical shift of the defect level. Because of the shown sharp decrease for $T > 0.1E_{\text{gap}}$ the coupled defect level will be shifted back into the conduction band. The peak of $\text{Im}\langle\langle a_i | a_i^\dagger \rangle\rangle_E$ is broadened in this case because of finite values for $\text{Im}\tilde{M}(E)$. This leads to a delocalization of the electron. This behavior is in good quantitative agreement with the experiment, where the spectrum connected with the electron capture disappears for $T > 6$ K.

V. ER DEFECT CASE

In the case of the Er ion we are interested in a microscopic picture of energetic lowering of the defect level. Because the Er^{3+} orbital is derived from a $4f$ configuration it is more strongly localized than the Gd orbital considered in the preceding section. Therefore we choose a weaker transfer coupling. The double occupancy of this level is excluded at low temperatures by a large Coulomb repulsion. This leads in our model to a term $H_U = U a_1^\dagger a_2^\dagger a_2 a_1$. We consider the limit $U \rightarrow \infty$ by introducing a Bose field with the operators b_0^\dagger and b_0 , which obeys the constraint

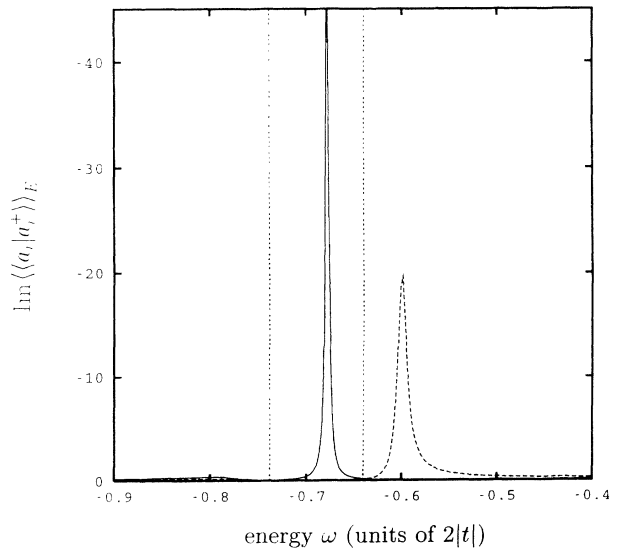


FIG. 3. Imaginary part of the Green function of the defect states for the model of the electron capture in the Gd case. $\tilde{\varepsilon}_0 + \mu = -0.56$; $t_d = 0.25$; $\mu = -0.72$; $kT = 0$. —, $\lambda = 0.25$; - - - -, $\lambda = 0$; ·····, band edges of the band gap.

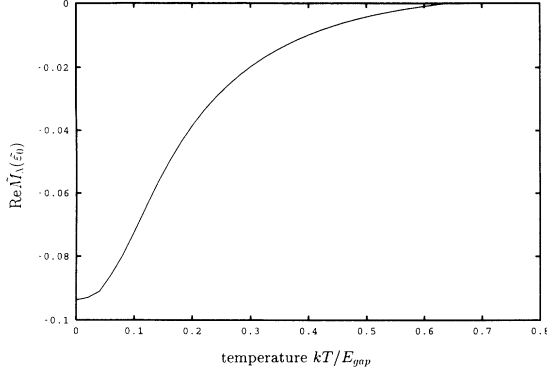


FIG. 4. Temperature dependency of the self-energy term $\text{Re}\tilde{M}_\lambda(\omega = \tilde{\epsilon}_0)$. $\tilde{\epsilon}_0 + \mu = -0.58$; $t_d = 0.25$; $\lambda = 0.25$.

$$b_0^\dagger b_0 + \sum_{i=1,2} a_i^\dagger a_i = 1. \quad (44)$$

Because H_λ conserves the number of defect electrons only the transfer term of our Hamiltonian has to be modified to be consistent with the restriction (44)

$$H = H_0 + H'_{t_d} + H_\lambda, \quad (45)$$

$$H'_{t_d} = t_d \sum_{\kappa} [\xi_{1t_d}(\kappa) c_\kappa b_0^\dagger a_1 + \xi_{2t_d}(\kappa) c_\kappa^\dagger b_0^\dagger a_2 + \text{H.c.}]. \quad (46)$$

In this section we calculate the Green function of the real defect level which is defined by $\langle\langle b_0^\dagger a_i | a_i^\dagger b_0 \rangle\rangle_E$.¹² The relevant observable of this section is $A = b_0^\dagger a_i$, in agreement with the Hilbert space restricted by Eq. (44). With the use of Mori's formalism we calculate the Green function up to terms of second order in $w = \lambda, t_d$. The corresponding terms of the expansion of the thermal expectation values are given in the Appendix. This series contains thermal expectation values of the undisturbed system, which is defined by the limit $U \rightarrow \infty$ of $H_0 + H_U$.

To determine ω_0 and $\tilde{M}(E)$ we use $\mathcal{L}b_0^\dagger a_i$, which yields

$$\mathcal{L}^0 b_0^\dagger a_i = -\tilde{\epsilon}_0 b_0^\dagger a_i, \quad (47)$$

$$\begin{aligned} \mathcal{L}'^{t_d} b_0^\dagger a_i = & -t_d \sum_{\kappa} \left[\xi_{1t_d}(\kappa) \left(\delta_{i,1} c_\kappa b_0^\dagger b_0 - a_1^\dagger c_\kappa a_i \right) \right. \\ & \left. + \xi_{2t_d}(\kappa) \left(\delta_{i,2} c_\kappa b_0^\dagger b_0 - a_2^\dagger c_\kappa a_i \right) \right], \end{aligned} \quad (48)$$

$$\begin{aligned} \mathcal{L}^\lambda b_0^\dagger a_i = & -\lambda \sum_{\kappa, \kappa'} \left(c_\kappa^\dagger c_{\kappa'} + c_{\kappa'}^\dagger c_\kappa \right) b_0^\dagger \\ & \times \left[\xi_0(\kappa) \xi_1(\kappa') \left(\delta_{i,2} a_2 - \delta_{i,1} a_1 \right) \right. \\ & \left. + \xi_0(\kappa) \xi_2(\kappa') \left(\delta_{i,2} a_1 + \delta_{i,1} a_2 \right) \right]. \end{aligned} \quad (49)$$

To obtain ω_0 [see Eq. (27)] we use

$$\left(\mathcal{L}^0 b_0^\dagger a_i | b_0 a_i \right) = -\tilde{\epsilon}_0, \quad (50)$$

$$\left(\mathcal{L}'^{t_d} b_0^\dagger a_i | b_0 a_i \right) = -t_d \sum_{\kappa} \left[\xi_{1t_d}(\kappa) \langle a_1^\dagger b c_\kappa \rangle_T (\delta_{i,1} - 1) + \xi_{2t_d}(\kappa) \langle a_2^\dagger b c_\kappa \rangle_T (\delta_{i,2} - 1) \right], \quad (51)$$

$$\begin{aligned} \left(\mathcal{L} b_0^\dagger a_i | b_0 a_i \right) = & -\lambda \sum_{\kappa, \kappa'} \xi_0(\kappa) \xi_1(\kappa') \times \left\langle \left(c_\kappa^\dagger c_{\kappa'} + c_{\kappa'}^\dagger c_\kappa \right) \left[b_0^\dagger b_0 (\delta_{i,2} - \delta_{i,1}) + a_2^\dagger a_2 \delta_{i,2} - a_1^\dagger a_1 \delta_{i,1} \right] \right\rangle_T \\ & + \xi_0(\kappa) \xi_2(\kappa') \left\langle \left(c_\kappa^\dagger c_{\kappa'} + c_{\kappa'}^\dagger c_\kappa \right) \left(\delta_{i,1} a_1^\dagger a_2 + \delta_{i,2} a_2^\dagger a_1 \right) \right\rangle_T. \end{aligned} \quad (52)$$

The thermal expectation values are determined to first order in w . Thereby the constraint (44) is reflected in $\bar{n}_E = \langle a_i^\dagger a_i \rangle_T = [\exp(\beta \tilde{\epsilon}_0) + 2]^{-1}$ and $\langle a_1^\dagger a_2^\dagger a_2 a_1 \rangle_T = 0$. The static value of the Mori scalar product is given by

$$\left(b_0^\dagger a_i | b_0^\dagger a_i \right) = 1 - \langle a_i^\dagger a_i \rangle_T. \quad (53)$$

The second order terms of the expansion of $\langle a_i^\dagger a_i \rangle_T$ yield

$$\langle a_i^\dagger a_i \rangle = \bar{n}_E + \langle a_i^\dagger a_i \rangle_T^1 + \langle a_i^\dagger a_i \rangle_T^2 + O(w^3), \quad (54)$$

$$\langle a_i^\dagger a_i \rangle^1 = 0 \quad (55)$$

$$\begin{aligned} \langle a_i a_i \rangle^2 = & t_d^2 \sum_{\kappa} \frac{\xi_E^2(\kappa)}{\tilde{\epsilon}_\kappa - \tilde{\epsilon}_0} \frac{1}{2} [f(\tilde{\epsilon}_\kappa, T) + 1] \beta \bar{n}_E \bar{n}_{SB} \\ & + \lambda^2 \sum_{\kappa, \kappa'} \frac{\xi_0^2(\kappa) \xi_E^2(\kappa') + \xi_E^2(\kappa) \xi_0^2(\kappa')}{\tilde{\epsilon}_\kappa - \tilde{\epsilon}_{\kappa'}} f(\tilde{\epsilon}_\kappa, T) \\ & \times [1 - f(\tilde{\epsilon}_{\kappa'}, T)] \beta \bar{n}_E \bar{n}_{SB}, \end{aligned} \quad (56)$$

$$\bar{n}_{SB} = \langle b_0^\dagger b_0 \rangle_T^0 = 1 - 2\bar{n}_E. \quad (57)$$

In the Er case charge fluctuations are not measured, whence, because of its proportionality to $\bar{n}_E \bar{n}_{SB}$, we can neglect the term $\langle a_i^\dagger a_i \rangle_T^2$ at low temperatures.

This yields for ω_0

$$\begin{aligned} \omega_0 = & -\tilde{\epsilon}_0 + \frac{1}{\bar{n}_E + \bar{n}_{SB}} \left\{ t_d^2 \sum_{\kappa} \frac{\xi_{Et_d}^2(\kappa)}{\tilde{\epsilon}_0 - \tilde{\epsilon}_{\kappa}} \{ \bar{n}_E [1 - f(\tilde{\epsilon}_{\kappa}, T)] - \bar{n}_{SB} f(\tilde{\epsilon}_{\kappa}, T) \} \right. \\ & \left. + \lambda^2 \sum_{\kappa, \kappa'} \frac{\xi_0^2(\kappa) \xi_E^2(\kappa') + \xi_E^2(\kappa) \xi_0^2(\kappa')}{\tilde{\epsilon}_{\kappa} - \tilde{\epsilon}_{\kappa'}} f(\tilde{\epsilon}_{\kappa'}, T) [1 - f(\tilde{\epsilon}_{\kappa}, T)] 2\bar{n}_E \right\}. \end{aligned} \quad (58)$$

The self-energy terms \tilde{M}_{λ} and \tilde{M}_{t_d} are determined to second order in w ,

$$\tilde{M}_{t_d}(E) = t_d^2 \frac{1}{\bar{n}_E + \bar{n}_{SB}} \sum_{\kappa} \frac{\xi_{Et_d}^2(\kappa)}{E - \tilde{\epsilon}_{\kappa}} \left(\frac{1}{2} \bar{n}_{SB} + \bar{n}_E \right), \quad (59)$$

$$\tilde{M}_{\lambda}(E) = \lambda^2 \frac{1}{\bar{n}_E + \bar{n}_{SB}} \sum_{\kappa, \kappa'} \frac{\xi_0^2(\kappa) \xi_E^2(\kappa') + \xi_E^2(\kappa) \xi_0^2(\kappa')}{E - \tilde{\epsilon}_0 - \tilde{\epsilon}_{\kappa'} + \tilde{\epsilon}_{\kappa}} \{ f(\tilde{\epsilon}_{\kappa}, T) [1 - f(\tilde{\epsilon}_{\kappa'}, T)] \bar{n}_{SB} + f(\tilde{\epsilon}_{\kappa'}, T) [1 - f(\tilde{\epsilon}_{\kappa}, T)] \bar{n}_E \}. \quad (60)$$

Thus finally we obtain for the Green function of the real defect states

$$\langle \langle b_0^{\dagger} a_i | a_i^{\dagger} b_0 \rangle \rangle_E = \frac{1}{2\pi} \frac{\bar{n}_E + \bar{n}_{SB}}{E + \omega_0 - [\tilde{M}_{t_d}(E) \tilde{M}_{\lambda}(E)]}. \quad (61)$$

Because the double occupancy of the defect level is excluded in this model for the Er^{3+} case the significant changes of the symmetry according to the defect occupation number as shown in the Gd case cannot appear. For that reason the Jahn-Teller coupling is effective for the defect level within the energy range below μ . This is inappropriate for the description of Er^{3+} . In Fig. 5 the imaginary part of the Green function is shown for $\tilde{\epsilon}_0 = -1.5$ with the parameters $t_d = 0.1$, $\lambda = 0$ (dotted line), and $\lambda = 0.2$ (full line). Obviously the Jahn-Teller coupling leads to an energetic lowering of the defect level as it was already derived within the molecular model.

VI. SUMMARY AND CONCLUDING REMARKS

We have considered a transfer coupling and electronic correlation effects, which establish a Jahn-Teller-like coupling of degenerate defect levels to a mixed-valent semi-

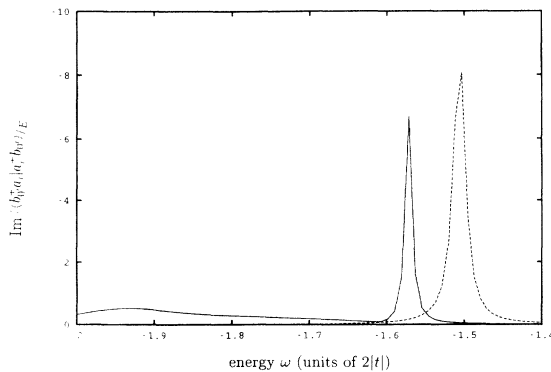


FIG. 5. Imaginary part of the Green's function of the real defect states in the model of the energetic lowering of the Er defect level. $\epsilon_0 = \tilde{\epsilon}_0 + \mu = -1.5$; $t_d = 0.1$; $kT = 0$; $\mu = -0.72$. —, $\lambda = 0.2$; ····, $\lambda = 0$.

conductor. In this model electronic excitations between symmetrized states of the surrounding take on the role which normally is played by distortions of the ionic configuration. In the host crystal SmB_6 this mechanism is more probable than the conventional one, because it takes advantage of the low energetic electronic excitations ($E_{\text{gap}} \sim 3 - 4$ meV).

Within our model the electron capture proposed to explain ESR measurements for $\text{SmB}_6:\text{Gd}$ can be explained in the following way: If the uncoupled defect level is lying within the conduction band near the band edge of the gap, the correlation coupling leads for $\lambda > \lambda_c$ to an “effective state” within the band gap. The conduction band electron introduced by the Gd^{3+} ion can be captured within this state. With increasing temperature this state is shifted back into the conduction band where the electron is delocalized because of the transfer coupling. This is in agreement with experimental results.⁴ Because of the transfer coupling we also expect contributions of the band states to this effective band-gap state. This will be examined in further work.

In the case of an Er^{3+} ion we took into account the prohibition of the doubly occupied defect state caused by a strong Coulomb repulsion. The correlation coupling leads to an energetic lowering of the defect level as was suggested by a molecular model to explain ESR measurements.

Within our model we have examined various microscopic coupling types, which differ in the degree of participation of the localized Sm $4f$ states in the coupled electronic transitions. Our result is that the energetic lowering is strongest when the defect states interact with transitions between A_{1g} and E_g states of the surrounding, both of which are composed of Sm $4f$ states. This is a result of the large density of low energetic excitations of predominantly $4f$ character in SmB_6 . This “soft” surrounding is characterized by the small band gap and the sharp maxima of the $4f$ partial density of states at the corresponding band edges. The dominant role of the Sm $4f$ states in the coupling mechanism is also confirmed by an approximate calculation of the coupling constant, which revealed higher λ values for the coupling to the localized states than to the delocalized states of the defect surrounding.

In further work we plan to examine the effects of the

unconventional Jahn-Teller coupling on the band states and on thermal properties of the doped semiconductor.

ACKNOWLEDGMENT

The authors thank the Deutsche Forschungsgemeinschaft for financial support.

APPENDIX A: APPENDIX

To calculate thermal expectation values like $\langle A \rangle_T^{H_0+W}$ to terms of second order in the perturbation W we made use of the expansion

$$\langle A \rangle_T^{H_0+W} = \langle A \rangle_T^0 + \langle A \rangle_T^1 + \langle A \rangle_T^2 + O(w^3), \quad (\text{A1})$$

with

$$\langle A \rangle_T^0 = \langle A \rangle_T^{H_0}, \quad (\text{A2})$$

$$\langle A \rangle_T^1 = \left\langle \int_0^\beta d\beta' W(\beta') \left(\langle A \rangle_T^{H_0} - A \right) \right\rangle_T^{H_0}, \quad (\text{A3})$$

$$\begin{aligned} \langle A \rangle_T^2 = & \left\langle \int_0^\beta d\beta' \int_0^{\beta'} d\beta'' W(\beta') W(\beta'') \left(A - \langle A \rangle_T^{H_0} \right) \right\rangle_T^{H_0} \\ & + \left\langle \int_0^\beta d\beta' W(\beta') \right\rangle_T^{H_0} \\ & \times \left\langle \int_0^\beta d\beta' W(\beta') \left(A - \langle A \rangle_T^{H_0} \right) \right\rangle_T^{H_0}, \quad (\text{A4}) \end{aligned}$$

$$W(\beta) = \exp(\beta H_0) W \exp(-\beta H_0).$$

β is the inverse temperature, which is multiplied by the Boltzmann constant.

¹B. Batlogg, P. H. Schmidt, and J. M. Rowell, in *Valence Fluctuations in Solids*, edited by L. M. Falicov, W. Hanke, and M. B. Maple (North-Holland, Amsterdam, 1981).

²G. Travaglini and P. Wachter, *Phys. Rev. B*, **29**, 893 (1984).

³J. W. Allen and R. M. Martin, *J. Phys. Colloq. (Paris)* **41**, C5-171 (1980).

⁴G. Wiese, H. Schäffer, and B. Elschner, *Europhys. Lett.* **11**, 791 (1990).

⁵H. Sturm, B. Elschner, and K. H. Höck, *Phys. Rev. Lett.* **54**, 1291 (1985).

⁶P. A. Alekseev, A. S. Ivanov, B. Dorner, H. Schober, K. A. Kikoin, A. S. Mishchenko, V. N. Lazukov, E. S. Konovalova, Y. B. Paderno, A. Y. Romyantsev and I. P. Sadikov, *Europhys. Lett.* **10**, 457 (1989).

⁷C. Weber, E. Sigmund, and M. Wagner, *Phys. Rev. Lett.* **55**, 1645 (1985).

⁸C. Weber, E. Sigmund and M. Wagner, *Phys. Status Solidi B* **138**, 661 (1986); **141**, 529 (1987).

⁹P. W. Anderson, *Phys. Rev.* **124**, 41 (1961).

¹⁰Zheng Hang, *J. Phys. C* **21**, 2351 (1988).

¹¹S. E. Barnes, *J. Phys. F* **6**, 1375 (1976).

¹²P. Coleman, *Phys. Rev. B* **29**, 3035 (1983).

¹³P. Fulde, J. Keller, and G. Zwicknagl, in *Solid State Physics: Advances in Research and Applications*, edited by H. Ehrenreich, F. Seitz, and D. Turnbull (Academic, New York, 1988), Vol. 41, p. 1.

¹⁴M. Wagner and J. Vázquez-Márquez, *J. Phys. A* **21**, 4377 (1988).